

Rhodium Cluster Complexes Containing Bridging Phenylgermanium Ligands

Richard D. Adams* and Jack L. Smith, Jr.

Department of Chemistry and Biochemistry, University of South Carolina, Columbia, South Carolina 29208

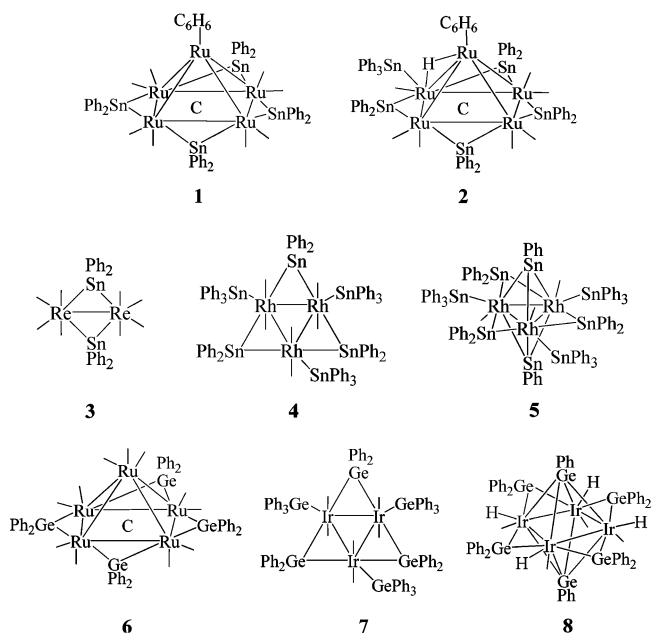
Received March 10, 2005

The reaction of $\text{Rh}_4(\text{CO})_{12}$ with Ph_3GeH at 97 °C has yielded the first rhodium cluster complexes containing bridging germylene and germylyne ligands: $\text{Rh}_8(\text{CO})_{12}(\mu_4\text{-GePh})_6$, **9**, and $\text{Rh}_3(\text{CO})_5(\text{GePh}_3)(\mu\text{-GePh}_2)_3(\mu_3\text{-GePh})(\mu\text{-H})$, **10**. When the reaction is performed under hydrogen, the yield of **9** is increased to 42% and no **10** is formed. Compound **9** contains a cluster of eight rhodium atoms arranged in the form of a distorted cube. There are six $\mu_4\text{-GePh}$ groups bridging each face of this distorted cube. Four of the rhodium atoms have two terminal carbonyl ligands, while the remaining four rhodium atoms have only one carbonyl ligand. Compound **10** contains a triangular cluster of three rhodium atoms with one terminal GePh_3 ligand, three bridging GePh_2 ligands, and one triply bridging GePh ligand. There is also one hydrido ligand that is believed to bridge one of the Rh–Ge bonds. Compound **9** reacted with PPhMe_2 at 25 °C to give the tetraphosphine derivative $\text{Rh}_8(\text{CO})_8(\text{PPhMe}_2)_4(\mu_4\text{-GePh})_6$, **11**. The structure of **11** is similar to **9** except that a PPhMe_2 ligand has replaced a carbonyl ligand on each the four $\text{Rh}(\text{CO})_2$ groups. Compound **10** reacted with CO at 68 °C to give the complex $\text{Rh}_3(\text{CO})_6(\mu\text{-GePh}_2)_3(\mu_3\text{-GePh})$, **12**. Compound **12** is formed by the loss of the hydrido ligand and the terminal GePh_3 ligand from **10** and the addition of one carbonyl ligand. All compounds were fully characterized by IR, NMR, elemental, and single-crystal X-ray diffraction analyses.

Introduction

In recent studies we have shown that Ph_3SnH is an excellent reagent for the introduction of bridging SnPh_2 ligands into polynuclear transition metal cluster complexes in a process that results in the elimination of benzene.¹ For example, the reaction of $\text{Ru}_5(\text{CO})_{12}(\text{C}_6\text{H}_6)(\mu_5\text{-C})$ with $\text{Ph}_3\text{-SnH}$ leads to the formation of two tin-rich compounds, $\text{Ru}_5(\text{CO})_8(\text{C}_6\text{H}_6)(\mu\text{-SnPh}_2)_4(\mu_5\text{-C})$, **1** (Chart 1), and $\text{Ru}_5(\text{CO})_7(\text{C}_6\text{H}_6)(\mu\text{-SnPh}_2)_4(\text{SnPh}_3)(\mu_5\text{-C})(\mu\text{-H})$, **2**.¹ The reaction of $\text{Re}_2(\text{CO})_8[\mu\text{-C}(\text{H})=\text{C}(\text{H})\text{Bu}^n]$ with Ph_3SnH yielded the complex $\text{Re}_2(\text{CO})_8(\mu\text{-SnPh}_2)_2$, **3**, with two bridging SnPh_2 ligands across a single Re–Re bond.² Rhodium and iridium are even more effective than ruthenium and rhenium in these tin addition reactions. The reaction of $\text{Rh}_4(\text{CO})_{12}$ with Ph_3SnH

Chart 1



* Author to whom correspondence should be addressed. E-mail: Adams@mail.chem.sc.edu.

- (1) (a) Adams, R. D.; Captain, B.; Fu, W.; Smith, M. D. *Inorg. Chem.* **2002**, *41*, 5593. (b) Adams, R. D.; Captain, B.; Fu, W.; Smith, M. D. *Inorg. Chem.* **2002**, *41*, 2302.
 (2) Adams, R. D.; Captain, B.; Johansson, M.; Smith, J. L. *J. Am. Chem. Soc.* **2005**, *127*, 488.

has yielded the trirhodium cluster complexes $\text{Rh}_3(\text{CO})_6(\mu\text{-SnPh}_2)_3(\text{SnPh}_3)_3$, **4**, and $\text{Rh}_3(\text{CO})_3(\text{SnPh}_3)_3(\mu\text{-SnPh}_2)_3(\mu_3\text{-SnPh})_2$, **5**, that contain six and eight tin ligands, respectively; the latter compound contains the first examples of triply bridging SnPh ligands.³

We have also shown that Ph_3GeH can also engage in multiple addition reactions to ruthenium and iridium cluster complexes to yield complexes with bridging GePh_2 ligands such as $\text{Ru}_5(\text{CO})_{11}(\mu\text{-GePh}_2)_4(\mu_5\text{-C})$, **6**,⁴ $\text{Ir}_3(\text{CO})_6(\mu\text{-GePh}_2)_3\text{-}(\text{GePh}_3)_3$, **7**,⁵ and $\text{Ir}_4(\text{CO})_4\text{H}_4(\mu\text{-GePh}_2)_4(\mu_4\text{-GePh})_2$, **8**.⁵ Compound **8** contains two quadruply bridging GePh ligands.

We have now investigated the reaction of $\text{Rh}_4(\text{CO})_{12}$ with Ph_3GeH and have obtained the first examples of rhodium carbonyl cluster complexes containing bridging GePh_2 and GePh ligands. These results are reported herein.

Experimental Section

General Data. All reactions were performed under a nitrogen atmosphere. Reagent grade solvents were dried by the standard procedures and were freshly distilled prior to use. Infrared spectra were recorded on a Thermo-Nicolet Avatar 360 FT-IR spectrophotometer. ¹H NMR spectra were recorded on a Mercury 300 spectrometer operating at 300.1 MHz. ³¹P{¹H} NMR spectra were recorded on a Varian Mercury 400 spectrometer operating at 161.9 MHz and were externally referenced against 85% *ortho*- H_3PO_4 . Elemental analyses were performed by Desert Analytics (Tucson, AZ). Product separations were performed by TLC in air on Analtech 0.5 mm silica gel 60 Å F_{254} glass plates. $\text{Rh}_4(\text{CO})_{12}$ was purchased from Strem Chemicals, Inc. Ph_3GeH and PPhMe_2 were purchased from Aldrich and were used without further purification.

Reaction of $\text{Rh}_4(\text{CO})_{12}$ with Ph_3GeH . Ph_3GeH (125 mg, 0.410 mmol) was added to a solution of $\text{Rh}_4(\text{CO})_{12}$ (30 mg, 0.040 mmol) in heptane. The reaction mixture was heated to reflux for 3 h. After cooling, the solvent was removed in vacuo, and the products were separated by TLC using a 2:1 hexane/methylene chloride solvent mixture to yield in order of elution 10.0 mg (12% yield) of green $\text{Rh}_8(\text{CO})_{12}(\mu_4\text{-GePh})_6$, **9**, and 11.3 mg (18% yield) of red $\text{Rh}_3(\text{CO})_5\text{-}(\text{GePh}_3)(\mu\text{-GePh}_2)_3(\mu_3\text{-GePh})(\mu\text{-H})$, **10**. Spectral data for **9**: IR (ν_{CO} ; cm^{-1} in hexane) 2031 (s), 2003 (m); ¹H NMR (CD_2Cl_2 in ppm) $\delta = 7.4\text{--}7.8$ (m, 30 H, Ph). Anal. Calcd: C, 28.01; H, 1.47. Found: C, 28.55; H, 1.68. MS (m/z): 2057, M^+ . Spectral data for **10**: IR (ν_{CO} ; cm^{-1} in hexane) 2054 (s), 2034 (s), 2016 (m), 2007 (m), 2001 (m); ¹H NMR (CD_2Cl_2 in ppm) $\delta = 6.8\text{--}7.6$ (m, 50 H, Ph), -10.42 (dt, 1 H, $\mu\text{-H}$, ¹ $J_{\text{Rh-H}} = 17$ Hz, ² $J_{\text{Rh-H}} = 2$ Hz). Anal. Calcd: C, 49.29; H, 3.25. Found: C, 48.95; H, 3.36 H.

Improved Route to **9.** Ph_3GeH (125 mg, 0.410 mmol) was added to a solution of $\text{Rh}_4(\text{CO})_{12}$ (30 mg, 0.040 mmol) in heptane. The reaction mixture was heated to reflux under a slow purge of H_2 for 3 h. After the solvent was removed in vacuo, the product **9** was separated by TLC by using a 2:1 hexane/methylene chloride solvent mixture to give 35.2 mg (42% yield).

Synthesis of $\text{Rh}_8(\text{CO})_8(\text{PPhMe}_2)_4(\mu_4\text{-GePh})_6$, **11.** PPhMe_2 (4.2 μL , 0.030 mmol) was added to a solution of **9** (15 mg, 0.0073 mmol) in CH_2Cl_2 and stirred at room temperature for 30 min. The solvent was then removed in vacuo and the product washed with acetonitrile and recrystallized from THF/heptane to give 14.7 mg (80% yield) of $\text{Rh}_8(\text{CO})_8(\text{PPhMe}_2)_4(\mu_4\text{-GePh})_6$, **11**. Spectral data

for **11**: IR (ν_{CO} ; cm^{-1} in hexane) 1967 (vs), 1946 (w); ¹H NMR (CD_2Cl_2 in ppm) $\delta = 7.1\text{--}7.5$ (m, 50 H, Ph), 1.29 (d, 12 H, Me), ² $J_{\text{P-H}} = 9$ Hz), 1.30 (d, 12 H, Me, ² $J_{\text{P-H}} = 9$ Hz); ³¹P NMR (CD_2Cl_2 in ppm) $\delta = -2.30$ (d, 4 P, ¹ $J_{\text{P-Rh}} = 158$ Hz). Anal. Calcd: C, 35.11; H, 2.95. Found: C, 34.04; H, 2.82.

Synthesis of $\text{Rh}_3(\text{CO})_6(\mu\text{-GePh}_2)_3(\mu_3\text{-GePh})$, **12.** Compound **10** (9.7 mg, 0.0061 mmol) was dissolved in hexane and heated to reflux under a slow purge of CO for 3 h. The solvent was then removed in vacuo and the product separated using a 2:1 hexane/methylene chloride solvent mixture to give 7.5 mg (94% yield) of red $\text{Rh}_3\text{-}(\text{CO})_6(\mu\text{-GePh}_2)_3(\mu_3\text{-GePh})$, **12**. Spectral data for **12**: IR (ν_{CO} ; cm^{-1} in hexane) 2055 (m), 2030 (s), 2009 (vs), 1998 (s); ¹H NMR (CD_2Cl_2 in ppm) $\delta = 6.9\text{--}7.8$ (m, 35 H, Ph). Anal. Calcd: C, 44.11; H, 2.69. Found: C, 43.38; H, 2.64.

Crystallographic Analyses. Green crystals of **9** and red crystals of **10** and **12** were grown by slow evaporation of a CH_2Cl_2 /hexane solvent mixture at -18 °C. Green crystals **11** were grown from THF/heptane at room temperature. Each data crystal was glued onto the end of a thin glass fiber. X-ray intensity data were measured by using a Bruker SMART APEX CCD-based diffractometer using Mo K α radiation ($\lambda = 0.71073$ Å). The raw data frames were integrated with the SAINT+ program⁶ by using a narrow-frame integration algorithm. Corrections for Lorentz and polarization effects were also applied with SAINT+. An empirical absorption correction based on the multiple measurement of equivalent reflections was applied using the program SADABS. All structures were solved by a combination of direct methods and difference Fourier syntheses and refined by full-matrix least squares on F^2 using the SHELXTL software package.⁷ For **9**, **11**, and **12** all non-hydrogen atoms were refined with anisotropic displacement parameters. For **10** only the rhodium and germanium atoms were refined with anisotropic displacement parameters. All hydrogen atoms were placed in geometrically idealized positions and included as standard riding atoms during the least-squares refinements. Crystal data, data collection parameters, and results of the analyses are listed in Tables 1 and 2.

Compounds **9** and **10** crystallized in the monoclinic crystal system. The space groups $P2_1/c$ and $P2_1/n$, for **9** and **10**, respectively, were identified uniquely on the basis of the systematic absences in the intensity data. One molecule of hexane cocrystallized with **10** and was located and satisfactorily refined at 50% occupancy with isotropic displacement parameters. Compounds **11** and **12** crystallized in the triclinic crystal system. The space group $P\bar{1}$ was assumed and confirmed by the successful solution and refinement of the structures. For **11** there are two independent formula equivalents and one molecule of THF in the asymmetric unit.

Results and Discussion

As a result of our successful synthesis of a number of new iridium carbonyl cluster complexes containing phenylgermanium ligands from the reaction of $\text{Ir}_4(\text{CO})_{12}$ with Ph_3GeH ,⁵ we proceeded to investigate the reaction of $\text{Rh}_4(\text{CO})_{12}$ with Ph_3GeH . $\text{Rh}_4(\text{CO})_{12}$ was found to react with Ph_3GeH at 97 °C to yield what are now the first examples of rhodium carbonyl cluster complexes containing bridging germylene and germylene ligands: $\text{Rh}_8(\text{CO})_{12}(\mu_4\text{-GePh})_6$, **9**, and $\text{Rh}_3\text{-}(\text{CO})_5(\text{GePh}_3)(\mu\text{-GePh}_2)_3(\mu_3\text{-GePh})(\mu\text{-H})$, **10**, in 12% and

(3) Adams, R. D.; Captain, B.; Smith, J. L.; Hall, M. B.; Beddie, C. L.; Webster, C. E. *Inorg. Chem.* **2004**, *43*, 7576.

(4) Adams, R. D.; Captain, B.; Fu, W. *Inorg. Chem.* **2003**, *42*, 1328.

(5) Adams, R. D.; Captain, B.; Smith, J. L. *Inorg. Chem.* **2005**, *44*, 1413.

(6) SAINT+, version 6.2a; Bruker Analytical X-ray Systems, Inc.: Madison, WI, 2001.

(7) Sheldrick, G. M. SHELXTL, version 6.1; Bruker Analytical X-ray Systems, Inc.: Madison, WI, 1997.

Table 1. Crystallographic Data for Compounds **9** and **10**

	9	10
empirical formula	Rh ₈ Ge ₆ O ₁₂ C ₄₈ H ₃₀	Rh ₃ Ge ₅ O ₅ C ₆₅ H ₅₀ ^{1/2} C ₆ H ₁₄
fw	2057.54	1625.82
cryst system	monoclinic	monoclinic
lattice params		
<i>a</i> (Å)	13.2207(13)	13.1447(6)
<i>b</i> (Å)	21.769(2)	21.6775(10)
<i>c</i> (Å)	19.867(2)	23.6975(11)
α (deg)	90	90
β (deg)	94.127(3)	91.5960(10)
γ (deg)	90	90
<i>V</i> (Å ³)	5703.1(10)	6749.8(5)
space group	<i>P</i> 2 ₁ / <i>c</i>	<i>P</i> 2 ₁ / <i>c</i>
<i>Z</i>	4	4
ρ_{calc} (g cm ⁻³)	2.396	1.600
μ (Mo K α) (mm ⁻¹)	5.412	2.954
temp (K)	296	296
$2\theta_{\text{max}}$ (deg)	50.06	45.44
no. of observns	7392	5579
no. of params	667	397
goodness of fit	0.976	1.125
max shift in cycle	0.001	0.000
residuals: ^a <i>R</i> , <i>R</i> _w (<i>I</i> > 2 σ (<i>I</i>))	0.0369, 0.0684	0.1162, 0.2330
abs corr	SADABS	SADABS
max/min	0.897/0.613	1.000/0.887
largest peak (e/Å ³)	0.586	0.988

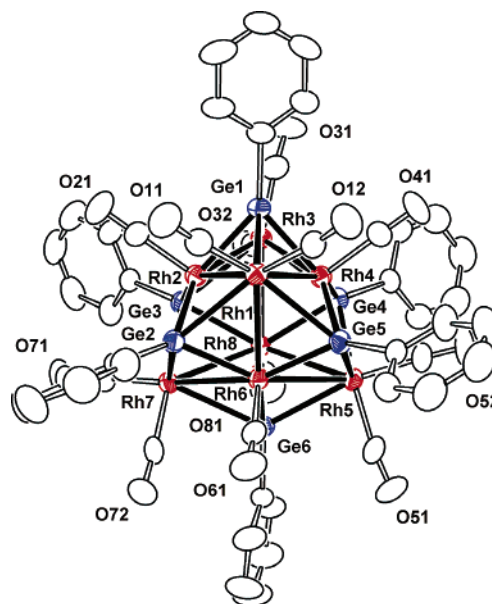
$$^a R = \sum_{hkl} (|F_o| - |F_c|) / \sum_{hkl} |F_o|; R_w = [\sum_{hkl} w(|F_o| - |F_c|)^2 / \sum_{hkl} w F_o^2]^{1/2}; w = 1/\sigma^2(F_o); GOF = [\sum_{hkl} w(|F_o| - |F_c|)^2 / (n_{\text{data}} - n_{\text{vars}})]^{1/2}.$$

Table 2. Crystallographic Data for Compounds **11** and **12**

	11	12
empirical formula	Rh ₈ Ge ₆ P ₄ O ₈ C ₇₆ H ₇₆ ·C ₄ H ₈ O	Rh ₃ Ge ₄ O ₆ C ₄₈ H ₃₅
fw	2570.16	1306.85
cryst system	triclinic	triclinic
lattice params		
<i>a</i> (Å)	14.1643(15)	11.5977(10)
<i>b</i> (Å)	14.4768(15)	12.9543(11)
<i>c</i> (Å)	24.717(3)	17.4276(15)
α (deg)	103.590(2)	98.147(2)
β (deg)	95.901(2)	94.135(2)
γ (deg)	104.608(2)	113.940(2)
<i>V</i> (Å ³)	4695.8(9)	2344.5(3)
space group	<i>P</i> $\bar{1}$	<i>P</i> $\bar{1}$
<i>Z</i>	2	2
ρ_{calc} (g cm ⁻³)	1.869	1.851
μ (Mo K α) (mm ⁻¹)	3.373	3.605
temp (K)	296	296
$2\theta_{\text{max}}$ (deg)	45.98	50.06
no. of observns	9257	6457
no. of params	967	550
goodness of fit	0.987	1.032
max shift in cycle	0.002	0.001
residuals: ^a <i>R</i> , <i>R</i> _w (<i>I</i> > 2 σ (<i>I</i>))	0.0841, 0.1993	0.0545, 0.1322
abs corr	SADABS	SADABS
max/min	1.000/0.459	0.835/0.493
largest peak (e/Å ³)	2.781	2.157

$$^a R = \sum_{hkl} (|F_o| - |F_c|) / \sum_{hkl} |F_o|; R_w = [\sum_{hkl} w(|F_o| - |F_c|)^2 / \sum_{hkl} w F_o^2]^{1/2}; w = 1/\sigma^2(F_o); GOF = [\sum_{hkl} w(|F_o| - |F_c|)^2 / (n_{\text{data}} - n_{\text{vars}})]^{1/2}.$$

18% yields, respectively. Both compounds were characterized by a combination of IR, ¹H NMR, elemental, and single-crystal X-ray diffraction analyses. Compound **9** was also characterized by mass spectral analysis. An ORTEP diagram of the molecular structure of **9** is shown in Figure 1. Selected intramolecular bond distances and angles are listed in Table 3. The structure of **9** consists of a distorted cube of eight rhodium atoms and six GePh groups that quadruply bridge each face. Quadruply bridging GeR ligands are known and include compound **8** as well as the nickel compound Ni₉(CO)₈(μ_4 -GeEt)₆.⁸ There are 12 Rh–Rh bonds ranging from 2.8208(7) to 2.9397(8) Å that link each of the four

**Figure 1.** ORTEP diagram of the molecular structure of Rh₈(CO)₁₂(μ_4 -GePh)₆, **9**, showing 40% thermal ellipsoid probability.**Table 3.** Selected Intramolecular Distances and Angles for Compound **9**^a

Bond Distances (Å)			
Rh(1)–Rh(2)	2.9234(8)	Rh(2)–Ge(2)	2.3928(8)
Rh(1)–Rh(4)	2.8208(7)	Rh(2)–Ge(3)	2.3679(9)
Rh(1)–Rh(6)	2.9237(8)	Rh(3)–Ge(1)	2.7197(9)
Rh(2)–Rh(3)	2.9274(7)	Rh(3)–Ge(3)	2.7102(9)
Rh(2)–Rh(7)	2.8304(8)	Rh(3)–Ge(4)	2.6052(9)
Rh(3)–Rh(4)	2.8657(8)	Rh(4)–Ge(1)	2.3882(9)
Rh(3)–Rh(8)	2.8258(8)	Rh(4)–Ge(4)	2.3580(8)
Rh(4)–Rh(5)	2.8862(8)	Rh(4)–Ge(5)	2.3833(9)
Rh(5)–Rh(6)	2.8237(7)	Rh(5)–Ge(4)	2.6815(9)
Rh(5)–Rh(8)	2.9331(8)	Rh(5)–Ge(5)	2.5704(9)
Rh(6)–Rh(7)	2.9397(8)	Rh(5)–Ge(6)	2.6797(9)
Rh(7)–Rh(8)	2.8923(7)	Rh(6)–Ge(2)	2.3424(9)
Rh(2)···Rh(4)	3.158(1)	Rh(6)–Ge(5)	2.3787(9)
Rh(2)···Rh(6)	3.247(1)	Rh(6)–Ge(6)	2.3793(9)
Rh(3)···Rh(8)	3.189(1)	Rh(7)–Ge(2)	2.6979(9)
Rh(4)···Rh(6)	3.201(1)	Rh(7)–Ge(3)	2.5490(9)
Rh(4)···Rh(8)	3.168(1)	Rh(7)–Ge(6)	2.5954(9)
Rh(6)···Rh(8)	3.264(1)	Rh(8)–Ge(3)	2.3794(9)
Rh(1)–Ge(2)	2.5959(9)	Rh(8)–Ge(4)	2.3529(9)
Rh(1)–Ge(5)	2.6284(9)	Rh(8)–Ge(6)	2.3523(9)
Rh(1)–Ge(6)	2.6340(9)	C–O(av)	1.14(3)
Rh(2)–Ge(1)	2.3302(9)		

Bond Angles (deg)			
Ge(2)–Rh(1)–Rh(2)	50.72(2)	Rh(1)–Rh(2)–Rh(3)	107.22(2)
Ge(2)–Rh(1)–Rh(4)	101.81(2)	Rh(2)–Rh(1)–Rh(4)	66.669(18)
Rh(1)–Ge(1)–Rh(2)	72.58(3)	Rh–C–O(av)	176(3)

^a Estimated standard deviations in the least significant figure are given in parentheses.

Rh(CO)₂ groups to three other Rh(CO) groups. In addition, the four Rh(CO) groups have a tetrahedral arrangement and contain six longer weak Rh–Rh interactions directly between themselves that range from 3.158(1) to 3.264(1) Å. An ORTEP diagram of the Rh₈ core of **9** is shown in Figure 2. The weak Rh–Rh interactions are represented by the open “bonds” between the metal atoms shown in Figure 2. The distortion in the Rh₈ core is most likely caused by the fact that four of the rhodium atoms have two carbonyl ligands

(8) Zebrowski, J. P.; Hayashi, R. K.; Bjarnason, A.; Dahl, L. F. *J. Am. Chem. Soc.* **1992**, *114*, 3121.

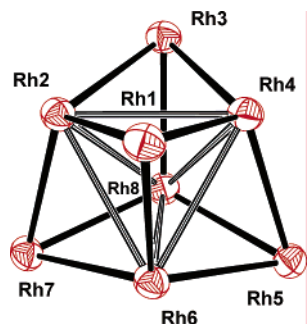


Figure 2. ORTEP diagram of the Rh₈ core of **9** showing 50% thermal ellipsoid probability. Open bonds represent the long weak Rh–Rh interactions not shown in Figure 1.

while the other four have only carbonyl ligand. The formation of the weak Rh–Rh interactions between the four Rh(CO) groups may be a result of their relative CO ligand deficiency. Each germanium atom is five coordinate which includes four Rh–Ge bonds. The Rh–Ge bond distances span a wide range, 2.3302(9)–2.7197(9) Å, and in general each germanium atom has two short Rh–Ge bonds and two long Rh–Ge bonds, e.g. Rh(1)–Ge(1) = 2.5959(9) Å, Rh(2)–Ge(1) = 2.3302(9) Å, Rh(3)–Ge(1) = 2.7197(9) Å, and Rh(4)–Ge(1) = 2.3882(9) Å; see Table 3. This can be attributed to the fact that the four rhodium atoms to which they are bonded are not arranged as a square. There are few examples of structurally characterized compounds that contain Rh–Ge bonds to compare with those in **9**. One is the compound [Me₂Si(NtBu)₂Ge]₄RhCl for which the four independent Rh–Ge bond distances were reported to be 2.3366(9), 2.3368(7), 2.3711(7), and 2.3756(8) Å.⁹

The total valence electron count for **9** is 114, which is 6 electrons less than the expected number of 120 for an cubical arrangement of eight metal atoms.¹⁰ There are many examples of structures of the type M₈(μ₄-E)₆ in the literature;¹¹ however, there is only one previous example of a cluster that contains an Rh₈ core with an electron count of 114 electrons, Rh₈(CO)₉[μ₄-P(C₅H₉)]₆.¹² Interestingly, when the reaction was performed under a hydrogen atmosphere, the yield of **9** was increased to 42% and no **10** was formed at all. No hydrogen is incorporated into the cluster. It may instead serve to assist in the removal of the phenyl groups from the germane with formation of benzene.¹

An ORTEP diagram of the molecular structure of **10** is shown in Figure 3. Selected intramolecular bond distances and angles are listed in Table 4. Compound **10** consists of a triangular arrangement of three rhodium atoms with one terminal GePh₃ ligand, three bridging GePh₂ ligands, and one triply bridging GePh ligand. This compound is isomor-

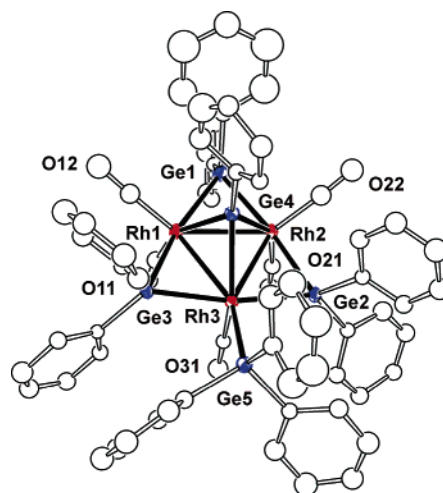


Figure 3. ORTEP diagram of the molecular structure of Rh₃(CO)₅(μ-GePh₂)₃(μ₃-GePh)(μ-H), **10**, showing 30% thermal ellipsoid probability. The hydrido ligand was not located crystallographically.

Table 4. Selected Intramolecular Distances and Angles for Compounds **10** and **12**^a

10		12	
Bond Distances (Å)			
Rh(1)–Rh(2)	2.824(2)	Rh(1)–Rh(2)	2.9101(8)
Rh(1)–Rh(3)	2.891(2)	Rh(1)–Rh(3)	2.8147(8)
Rh(2)–Rh(3)	2.857(2)	Rh(2)–Rh(3)	2.8610(8)
Rh(1)–Ge(1)	2.488(3)	Rh(1)–Ge(1)	2.4815(9)
Rh(1)–Ge(3)	2.522(3)	Rh(1)–Ge(3)	2.4762(9)
Rh(1)–Ge(4)	2.384(3)	Rh(1)–Ge(4)	2.4188(8)
Rh(2)–Ge(1)	2.462(3)	Rh(2)–Ge(1)	2.4783(9)
Rh(2)–Ge(2)	2.501(3)	Rh(2)–Ge(2)	2.4782(9)
Rh(2)–Ge(4)	2.384(3)	Rh(2)–Ge(4)	2.4157(9)
Rh(3)–Ge(2)	2.465(3)	Rh(3)–Ge(2)	2.4782(9)
Rh(3)–Ge(3)	2.476(3)	Rh(3)–Ge(3)	2.4794(9)
Rh(3)–Ge(4)	2.533(3)	Rh(3)–Ge(4)	2.4039(9)
Rh(3)–Ge(5)	2.480(3)	C–O(av)	1.13(2)
C–O(av)	1.18(7)		
Bond Angles (deg)			
Ge(1)–Rh(1)–Ge(3)	164.32(11)	Ge(1)–Rh(1)–Ge(3)	167.68(3)
Ge(4)–Rh(1)–Rh(3)	56.43(8)	Ge(4)–Rh(1)–Rh(3)	54.05(2)
Ge(1)–Rh(2)–Rh(3)	116.55(9)	Ge(1)–Rh(2)–Rh(3)	112.09(3)
Ge(2)–Rh(2)–Ge(4)	90.04(10)	Ge(2)–Rh(2)–Ge(4)	83.30(3)
Rh(1)–Ge(1)–Rh(2)	69.56(8)	Rh(1)–Ge(1)–Rh(2)	71.85(3)
Rh–C–O(av)	176(6)	Rh–C–O(av)	176(2)

^a Estimated standard deviations in the least significant figure are given in parentheses.

phous and isostructural with its iridium homologue, Ir₃(CO)₅-(GePh₃)(μ-GePh₂)₃(μ₃-GePh)(μ-H), that we recently reported.⁵ The Rh–Rh bond distances [range 2.824(2)–2.891(2) Å] are significantly longer than those in Rh₄(CO)₁₂ [2.6603(17)–2.7642 Å].¹³ We have previously shown that edge-bridging germanium and tin ligands produce lengthening effects on the M–M bonds that they bridge in related triangular rhodium and iridium cluster complexes.^{3,5} Fenske–Hall calculations on compound **4** have shown that this is due to very strong Rh–Sn interactions and weak Rh–Rh interactions. The hydrido ligand in **10** was not located crystallographically but is believed to bridge the Rh(3)–Ge(4) bond. The hydrido ligand in the related compound Ir₃(CO)₅(GePh₃)(μ-GePh₂)₃(μ₃-GePh)(μ-H) was located in a similar bridging position.⁵ The Rh(3)–Ge(4) bond [2.533-

(13) Farrugia, L. J. *J. Cluster Sci.* **2000**, *11*, 39.

- (9) Veith, M.; Müller, A.; Stahl, L.; Notzel, Jarczyk, M.; Huch, V. *Inorg. Chem.* **1996**, *35*, 3848.
- (10) (a) Lauher, J. W. *J. Am. Chem. Soc.* **1978**, *100*, 5305. (b) Burdett, J. K.; Miller, G. J. *J. Am. Chem. Soc.* **1987**, *109*, 4081.
- (11) (a) Lower, L. D.; Dahl, L. F. *J. Am. Chem. Soc.* **1976**, *98*, 5046. (b) Fenske, D.; Merzweiler, J. O. *Angew. Chem., Int. Ed. Engl.* **1988**, *27*, 1512. (c) Fenske, D.; Magull, J. Z. *Naturforsch., B: Chem. Sci.* **1990**, *45*, 121. (d) Fenske, D.; Krautscheid, M. M. *Angew. Chem., Int. Ed. Engl.* **1992**, *31*, 321. (e) Fenske, D.; Hachgenei, F. R. *Angew. Chem., Int. Ed. Engl.* **1984**, *23*, 982.
- (12) Arif, A. M.; Jones, R. A.; Heaton, D. E.; Nunn, C. M.; Schwab, S. T. *Inorg. Chem.* **1988**, *27*, 254.

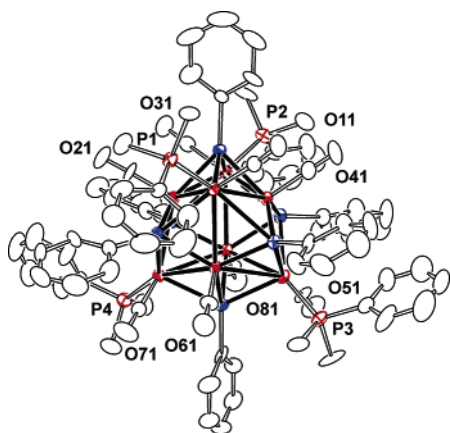


Figure 4. ORTEP diagram of the molecular structure of $\text{Rh}_8(\text{CO})_8(\text{PPhMe}_2)_4(\mu_4\text{-GePh})_6$, **11**, showing 30% thermal ellipsoid probability. The atom labeling scheme for the Rh_8Ge_6 core is similar to that of compound **9** in Figure 1.

Table 5. Selected Intramolecular Distances and Angles for Compound **11**^a

Bond Distances (Å)			
Rh(1)–Rh(2)	2.9423(18)	Rh(3)–Ge(1)	2.512(2)
Rh(1)–Rh(4)	2.8626(17)	Rh(3)–Ge(3)	2.795(2)
Rh(1)–Rh(6)	2.9525(18)	Rh(3)–Ge(4)	2.641(2)
Rh(2)–Rh(3)	2.8660(18)	Rh(4)–Ge(1)	2.424(2)
Rh(2)–Rh(7)	2.9397(18)	Rh(4)–Ge(4)	2.344(2)
Rh(3)–Rh(4)	2.9521(19)	Rh(4)–Ge(5)	2.378(2)
Rh(3)–Rh(8)	2.9561(19)	Rh(5)–Ge(4)	2.826(2)
Rh(4)–Rh(5)	2.9497(18)	Rh(5)–Ge(5)	2.614(2)
Rh(5)–Rh(6)	2.9377(17)	Rh(5)–Ge(6)	2.516(2)
Rh(5)–Rh(8)	2.8780(18)	Rh(6)–Ge(2)	2.374(2)
Rh(6)–Rh(7)	2.8689(18)	Rh(6)–Ge(5)	2.353(2)
Rh(7)–Rh(8)	2.9585(18)	Rh(6)–Ge(6)	2.437(2)
Rh(2)···Rh(4)	3.387(2)	Rh(7)–Ge(2)	2.812(2)
Rh(2)···Rh(6)	3.288(2)	Rh(7)–Ge(3)	2.639(2)
Rh(2)···Rh(8)	3.284(2)	Rh(7)–Ge(6)	2.522(2)
Rh(4)···Rh(6)	3.277(2)	Rh(8)–Ge(3)	2.349(2)
Rh(4)···Rh(8)	3.266(2)	Rh(8)–Ge(4)	2.369(2)
Rh(6)···Rh(8)	3.395(2)	Rh(8)–Ge(6)	2.419(2)
Rh(1)–Ge(1)	2.506(2)	Rh(1)–P(1)	2.301(4)
Rh(1)–Ge(2)	2.611(2)	Rh(3)–P(2)	2.296(5)
Rh(1)–Ge(5)	2.818(2)	Rh(5)–P(3)	2.305(5)
Rh(2)–Ge(1)	2.426(2)	Rh(7)–P(4)	2.289(5)
Rh(2)–Ge(2)	2.358(2)	C–O(av)	1.15(6)
Rh(2)–Ge(3)	2.381(2)		

Bond Angles (deg)			
Ge(2)–Rh(1)–Rh(2)	49.81(5)	Rh(1)–Rh(2)–Rh(3)	102.66(5)
Ge(2)–Rh(1)–Rh(4)	104.71(6)	Rh(2)–Rh(1)–Rh(4)	71.33(5)
Rh(1)–Ge(1)–Rh(2)	73.22(7)	Rh–C–O(av)	177(5)

^a Estimated standard deviations in the least significant figure are given in parentheses.

(3) Å] is significantly longer than the Rh(1)–Ge(4) and the Rh(2)–Ge(4) bonds [2.384(3) and 2.384(3) Å, respectively]. This lengthening effect is most likely due to the presence of the bridging hydrido ligand. The ¹H NMR spectrum of **10** exhibits a single resonance at –10.42 ppm with appropriate proton–rhodium coupling (¹J_{Rh–H} = 17 Hz, ²J_{Rh–H} = 2 Hz) and is consistent with this assignment.

Compound **9** reacted with PPhMe₂ at 25 °C to give the tetraphosphine derivative $\text{Rh}_8(\text{CO})_8(\text{PPhMe}_2)_4(\mu_4\text{-GePh})_6$, **11**, in 80% yield. An ORTEP diagram of the molecular structure of **11** is shown in Figure 4. Selected intramolecular bond distances and angles are listed in Table 5. Compound **11** was fully characterized by IR, ¹H and ³¹P NMR, elemental,

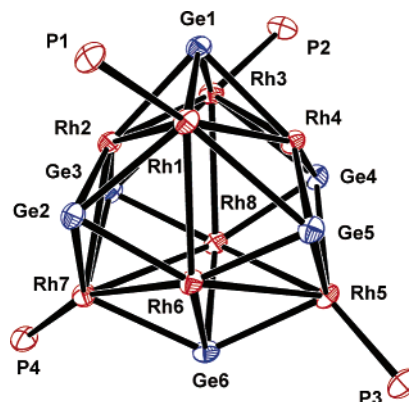
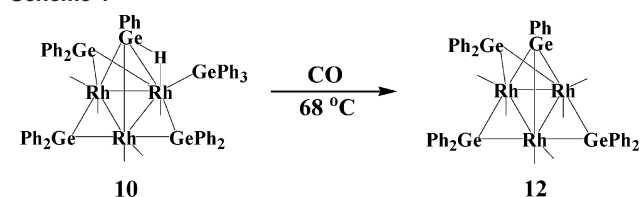


Figure 5. ORTEP diagram of the $\text{Rh}_8\text{Ge}_6\text{P}_4$ core of **11** showing 40% thermal ellipsoid probability.

Scheme 1



and single-crystal X-ray diffraction analyses. The structure of **11** is similar to **9** except that the four PPhMe₂ ligands have replaced four carbonyl groups, one from each of the four Rh(CO)₂ groups. An ORTEP diagram of the $\text{Rh}_8\text{Ge}_6\text{P}_4$ core of **11** is shown in Figure 5. If one ignores all phenyl groups, the molecule possesses an *S*₄ improper rotation axis that passes through the two atoms Ge(1) and Ge(6). In accord with this, the ³¹P NMR spectrum exhibits a single resonance at –2.30 ppm with appropriate coupling to rhodium, (¹J_{P–Rh} = 158 Hz) which is consistent with the presence of four equivalent PPhMe₂ groups. The ¹H NMR spectrum shows two resonances at 1.29 ppm (d, 12 H, Me, ²J_{P–H} = 9 Hz) and 1.30 ppm (d, 12 H, Me, ²J_{P–H} = 9 Hz) which can be attributed to the two inequivalent methyl groups on each of the four phosphorus atoms. The Rh–Rh bond distances in **11**, including all distances between the four Rh(CO) groups [3.277(2)–3.395(2) Å], are generally longer than those observed in the structure of **9**. This can be attributed to the increase in steric effects introduced by the replacement of the CO ligands with the bulkier phosphine ligands.

Compound **10** reacted with CO at 68 °C to give the complex $\text{Rh}_3(\text{CO})_6(\mu\text{-GePh}_2)_3(\mu_3\text{-GePh})$, **12**, in 94% yield; see Scheme 1. An ORTEP diagram of the molecular structure of **12** is shown in Figure 6. Selected intramolecular bond distances and angles are listed in Table 4. Compound **12** was fully characterized by IR, NMR, elemental, and single-crystal X-ray diffraction analyses. Compound **12** was formed by the loss of the hydrido ligand and the terminal GePh₃ ligand from **10** and the addition of one carbonyl ligand. The Rh–Rh distances in **12**, 2.8147(8), 2.8610(8), and 2.9101(8) Å, are similar to those in **10**. Interestingly, unlike **10** all three Rh–Ge distances to the triply bridging GePh ligand in **12** are similar in length, 2.4188(8), 2.4157(9), and 2.4039(9) Å.

The reaction of $\text{Rh}_4(\text{CO})_{12}$ with Ph₃GeH has yielded the first rhodium carbonyl cluster complexes **9** and **10** that

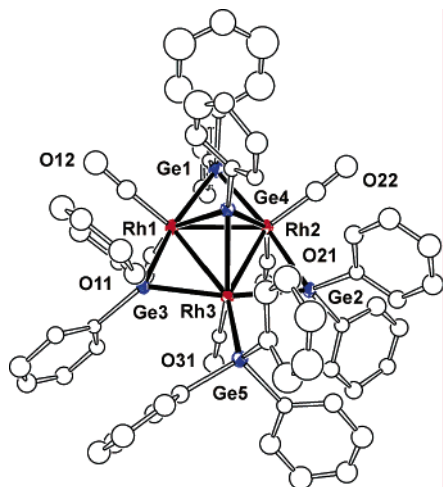


Figure 6. ORTEP diagram of the molecular structure of $\text{Rh}_3(\text{CO})_6(\mu\text{-GePh}_2)_3(\mu_3\text{-GePh})$, **12**, showing 30% thermal ellipsoid probability.

contain bridging germylene and germylyne ligands. Compound **9** is a high-nuclearity, eight metal complex containing quadruply bridging GePh germylyne ligands. Compound **10** has only three rhodium atoms with three edge bridging GePh_2 germylene ligands and one triply bridging GePh germylyne ligand. A compound similar to **10** was obtained from the

reaction of $\text{Ir}_4(\text{CO})_{12}$ with Ph_3GeH , but no iridium homologue of **9** has yet been reported. Compound **9** reacts with PPhMe_2 to give the CO ligand substitution product **11**. It seems likely that it will be possible to prepare additional rhodium cluster complexes containing bridging germylene and germylyne ligands in the future. Germanium has been shown to be a useful modifier of rhodium for applications in catalysis.¹⁴ Perhaps these new rhodium–germanium complexes can be used as precursors for new rhodium–germanium catalysts.

Acknowledgment. This research was supported by the Office of Basic Energy Sciences of the U.S. Department of Energy under Grant No. DE-FG02-00ER14980. We thank the USC NanoCenter for partial support of this work.

Supporting Information Available: CIF files for the structural analyses of **9–12**. This material is available free of charge via the Internet at <http://pubs.acs.org>.

IC050372E

- (14) (a) Lafaye, G.; Micheaud-Especel, C.; Montassier, C.; Marecot, P. *Appl. Catal., A* **2002**, *230*, 19. (b) Didillon, B.; Candy, J. P.; Lepepetier, F.; Ferretti, O. A.; Basset, J. M. *Stud. Surf. Sci. Catal.* **1993**, *78*, 147. (c) Lafaye, G.; Mihut, C.; Especel, C.; Marecot, P.; Amiridis, M. D. *Langmuir* **2004**, *20*, 10612.